



Article

Possible Contribution of Inflammation-Associated Hypoxia to Increased $K_{2P5.1}$ K^+ Channel Expression in $CD4^+$ T Cells of the Mouse Model for Inflammatory Bowel Disease

Kyoko Endo ^{1,2}, Hiroaki Kito ², Ryo Tanaka ¹, Junko Kajikuri ² , Satoshi Tanaka ¹ ,
Elghareeb E. Elboray ^{3,4}, Takayoshi Suzuki ³ and Susumu Ohya ^{2,*}

¹ Department of Pharmacology, Division of Pathological Sciences, Kyoto Pharmaceutical University, Kyoto 607-8414, Japan; kd16001@poppy.kyoto-phu.ac.jp (K.E.); rt.hk0304@gmail.com (R.T.); tanaka-s@mb.kyoto-phu.ac.jp (S.T.)

² Department of Pharmacology, Graduate School of Medical Sciences, Nagoya City University, Nagoya 467-8601, Japan; kito@med.nagoya-cu.ac.jp (H.K.); kajikuri@med.nagoya-cu.ac.jp (J.K.)

³ Department of Complex Molecular Chemistry, The Institute of Scientific and Industrial Research, Osaka University, Osaka 567-0047, Japan; elborayvip@yahoo.com (E.E.E.); tkyssuzuki@sanken.osaka-u.ac.jp (T.S.)

⁴ Faculty of Science, South Valley University, Qena 83523, Egypt

* Correspondence: sohya@med.nagoya-cu.ac.jp; Tel.: +81-52-853-8149

Received: 16 November 2019; Accepted: 17 December 2019; Published: 19 December 2019



Abstract: Previous studies have reported the up-regulation of the two-pore domain K^+ channel $K_{2P5.1}$ in the $CD4^+$ T cells of patients with multiple sclerosis (MS) and rheumatoid arthritis (RA), as well as in a mouse model of inflammatory bowel disease (IBD). However, the mechanisms underlying this up-regulation remain unclear. Inflammation-associated hypoxia is involved in the pathogenesis of autoimmune diseases, such as IBD, MS, and RA, and T cells are exposed to a hypoxic environment during their recruitment from inflamed tissues to secondary lymphoid tissues. We herein investigated whether inflammation-associated hypoxia is attributable to the increased expression and activity of $K_{2P5.1}$ in the splenic $CD4^+$ T cells of chemically-induced IBD model mice. Significant increases in hypoxia-inducible factor (HIF)-1 α transcripts and proteins were found in the splenic $CD4^+$ T cells of the IBD model. In the activated splenic $CD4^+$ T cells, hypoxia (1.5% O_2) increased $K_{2P5.1}$ expression and activity, whereas a treatment with the HIF inhibitor FM19G11 but not the selective HIF-2 inhibitor exerted the opposite effect. Hypoxia-exposed $K_{2P5.1}$ up-regulation was also detected in stimulated thymocytes and the mouse T-cell line. The class III histone deacetylase sirtuin-1 (SIRT1) is a downstream molecule of HIF-1 α signaling. We examined the effects of the SIRT1 inhibitor NCO-01 on $K_{2P5.1}$ transcription in activated $CD4^+$ T cells, and we found no significant effects on the $K_{2P5.1}$ transcription. No acute compensatory responses of $K_{2P3.1}$ – $K_{2P5.1}$ up-regulation were found in the $CD4^+$ T cells of the IBD model and the hypoxia-exposed T cells. Collectively, these results suggest a mechanism for $K_{2P5.1}$ up-regulation via HIF-1 in the $CD4^+$ T cells of the IBD model.

Keywords: K^+ channel; $K_{2P5.1}$; inflammatory bowel disease; $CD4^+$ T cell; hypoxia; HIF-1 α

1. Introduction

Alkaline pH-activated K^+ channels ($K_{2P5.1}$, 16.1, 17.1) belonging to the two-pore domain K^+ (K_{2P}) channel superfamily contribute to setting the resting potential and control of Ca^{2+} signaling, and they have also been implicated in inflammation and cancer development [1–3]. $K_{2P5.1}$ (also referred to TASK-2 and KCNK5) plays an important role in cell volume regulation, renal bicarbonate reabsorption,

and cancer cell proliferation [4–6]. $K_{2P5.1}$ expression and activity is up-regulated in the $CD4^+$ T cells of patients with autoimmune diseases such as rheumatoid arthritis (RA) [7], and multiple sclerosis (MS) [8] and those from inflammatory bowel disease (IBD) model mice [9]; however, the mechanisms that underly inflammatory response-mediated $K_{2P5.1}$ up-regulation in $CD4^+$ T cells remain unclear.

The dysregulated transcriptional, translational, and post-translational expression of K^+ channels is associated with the pathogenesis of immune and inflammatory disorders [10]. Three major K^+ channel subtypes—voltage-gated $K_V1.3$, Ca^{2+} -activated $K_{Ca3.1}$, and $K_{2P5.1}$ —have been extensively studied in T cells [7,8,11,12]. We recently reported the histone deacetylase (HDAC)-mediated up-regulation of $K_{Ca3.1}$ in the $CD4^+$ T cells of IBD model mice [13,14]. However, no significant changes were observed in the expression levels of $K_{2P5.1}$ transcripts following a treatment with selective class I HDAC inhibitors, suggesting that the mechanisms responsible for $K_{Ca3.1}$ and $K_{2P5.1}$ transcription in T cells under inflammatory conditions differ.

Hypoxia is linked to brain inflammation in MS patients [15], synovial inflammation in RA patients [16], and intestinal inflammation in IBD patients [17]. Hypoxia-inducible factors (HIFs) are heterodimeric transcriptional factors that consist of an oxygen-labile α subunit and a constitutively stable β subunit and that are involved in innate and adaptive immune activation. T cells are exposed to hypoxic conditions during their recruitment from inflamed tissues to secondary lymphoid tissues, such as the spleen and mesenteric lymph nodes, and HIF-1 α is strongly expressed in T cells that infiltrate the inflamed mucosa in IBD patients [18]. HIF-1 α plays a prominent role in the pathogenesis of inflammatory diseases by promoting inflammatory gene expression [19]. The leukocyte and myeloid cell-specific knockdown of HIF-1 α has been found to result in more severe colonic inflammation with increased levels of pro-inflammatory cytokines in dextran sulfate sodium (DSS)-induced IBD model mice [18,20–22], indicating that hypoxia underlies the polarization of inflammatory T cells such as type 1 T helper (Th1) and Th17 cells in inflamed tissues. The hypoxic microenvironment is responsible for the control of Ca^{2+} homeostasis through altered K^+ channel expression and function. For example, chronic hypoxia was reported to post-transcriptionally decrease the functional activity of the voltage-gated K^+ channel $K_V1.3$ by preventing forward trafficking from the trans-Golgi to the plasma membrane in T cells [23]. In contrast, an increase in the activity of $K_{2P5.1}$ was found to be induced under sustained hypoxia in B cells, and $K_{2P5.1}$ was found to be transcriptionally up-regulated via an HIF-1 α -mediated signaling pathway [24]. Yuan et al. reported that hypoxia enhanced $K_{2P5.1}$ protein expression in the carotid body [25].

Hypoxia-induced decreases in nicotinamide adenine dinucleotide (NAD^+) were shown to reduce the activity of the class III NAD^+ -dependent HDAC, and sirtuin-1 (SIRT1) [26]. Furthermore, SIRT1 was found negatively regulate inflammatory pathways such as signal transducer and activator of transcription-3 (STAT3), SMAD7, and nuclear factor (NF)- κ B [27], and it was also found to be down-regulated in IBD patients and IBD model mice [28]. However, SIRT1-mediated modifications to inflammation-associated ion channels have not yet been examined in detail.

In the present study, in order to elucidate the mechanisms that underly the increased $K_{2P5.1}$ activity in the inflammatory $CD4^+$ T cells of IBD model mice, we focused on the transcriptional regulation of $K_{2P5.1}$ by inflammation-associated hypoxia.

2. Results

2.1. Up-Regulation of HIF-1 α in Splenic $CD4^+$ T Cells of DSS-Induced IBD Model Mice

We assessed the expression levels of HIF-1 α in the splenic $CD4^+$ T cells of normal and IBD model mice. As shown in our previous study [9], the expression levels of $K_{2P5.1}$ and interferon (IFN)- γ transcripts in $CD4^+$ T cells were higher in IBD model mice than in normal mice ($n = 4$ mice for each group, $p = 0.0000$ and $p = 0.0002$ for $K_{2P5.1}$ and IFN - γ , respectively) (Supplementary Figure S1A,B). As shown in Figure 1A, the expression levels of HIF-1 α transcripts in splenic $CD4^+CD25^-$ T cells were approximately 50% higher in the IBD model mice than in the normal mice ($n = 4$, $p = 0.0052$).

HIF-2 α transcripts were less abundantly expressed in the CD4⁺CD25⁻ T cells of both groups, and no significant differences were found between the groups ($n = 4$, $p = 0.4439$) (Figure 1B). Immunoblots of HIF-1 α were performed with whole lysates of the CD4⁺ T cells. A band with a molecular weight of approximately 130 kDa that reacted with the anti-HIF-1 α antibody was observed in both groups (Figure 1C). Similar to previous studies [17–19,21,22], the summarized results showed that the protein expression levels of HIF-1 α in the CD4⁺ T cells were significantly higher in the IBD model mice than in the normal mice ($n = 4$, $p = 0.0083$) (Figure 1D). These results suggest that the CD4⁺ T cells of the IBD model were exposed to hypoxic conditions during their recruitment from the inflamed colon to the spleen, resulting in HIF-1 α being strongly expressed in inflammatory T cells.

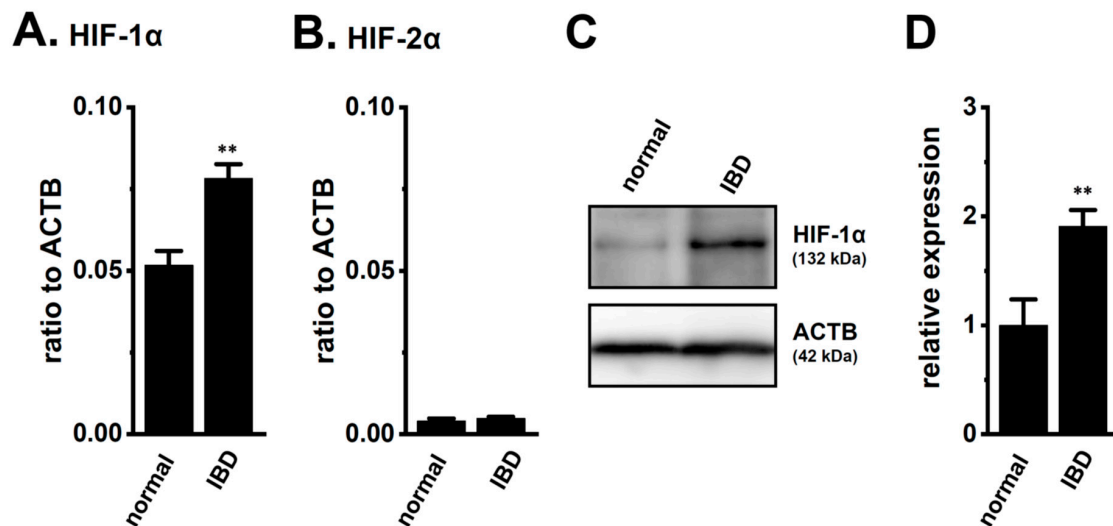


Figure 1. Increased expression of hypoxia-inducible factor (HIF)-1 α in the splenic CD4⁺ T cells of dextran sulfate sodium (DSS)-induced inflammatory bowel disease (IBD) model mice. (A,B) Real-time PCR assay for HIF-1 α (A) and -2 α (B) in the splenic CD4⁺CD25⁻ T cells of ‘normal’ and ‘IBD’ model mice ($n = 4$). Expression levels are shown as a ratio to β -actin (ACTB). (C,D) HIF-1 α protein expression (132 kDa) in the splenic CD4⁺ T cells of ‘normal’ and ‘IBD’ model mice. Protein lysates of the examined cells were probed by immunoblotting with anti-HIF-1 α (upper panel) and anti-ACTB (42 kDa, lower panel) antibodies on the same filter (C). Summarized results were obtained as the optical density of HIF-1 α and ACTB band signals (D). After compensation for the optical density of the HIF-1 α protein band signal with that of the ACTB signal, the HIF-1 α signal in ‘normal’ mice was expressed as 1.0 ($n = 4$). Results are expressed as means \pm SEM. **: $p < 0.01$ vs. normal mice (normal).

2.2. Enhancement of $K_{2p5.1}$ Transcription by the Exposure to Hypoxia (1.5% O_2) in Stimulated Splenic CD4⁺ T Cells of Mice

We recently demonstrated the up-regulation of $K_{2p5.1}$ with an increase in HIF-1 α expression in mouse splenic CD4⁺ T cells stimulated by concanavalin-A (Con-A) for 24–48 h [29]. Twenty-four hours after stimulation by Con-A, Con-A-stimulated CD4⁺ T cells were exposed to hypoxia (1.5% O_2) for an additional 24 h. The expression levels of $K_{2p5.1}$ transcripts were approximately 50% higher in the hypoxia-exposed CD4⁺ T cells ($p = 0.0246$) (Figure 2B) with the HIF-1 α up-regulation ($p = 0.0077$) (Figure 2A) than in those exposed to normoxia (20.8% O_2) ($n = 4$). Immunoblots of HIF-1 α were then obtained by using stimulated CD4⁺ T cells that were exposed to normoxia and hypoxia for 24 h. No significant differences were observed in the HIF-1 α -specific band signals (132 kDa) between both groups (Figure 2(Cc)). On the other hand, the stronger expression of the HIF-1 α proteins was noted in the hypoxia group exposed for 6 and 12 h (Figure 2(Ca,b)). It has been reported that HIF-1 α is continuously active even though HIF-1 α proteins are suppressed by long-term hypoxia [19]. In our previous study [9], immunoblots of $K_{2p5.1}$ were successfully performed by using a rabbit polyclonal anti- $K_{2p5.1}$ antibody that was purchased from Santa Cruz Biotechnology; however, this antibody has

since been discontinued. In the present study, we examined immunoblots of K_{2p}5.1 by using other commercially-available anti-K_{2p}5.1 antibodies under several experimental conditions; however, no signals of the K_{2p}5.1 proteins at approximately 45 kDa (predicted molecular weight) for the analysis of CD4⁺ T cell lysates in both groups were detected, and the detected band signals with different molecular weights were not disappeared by the preincubation with excess antigens.

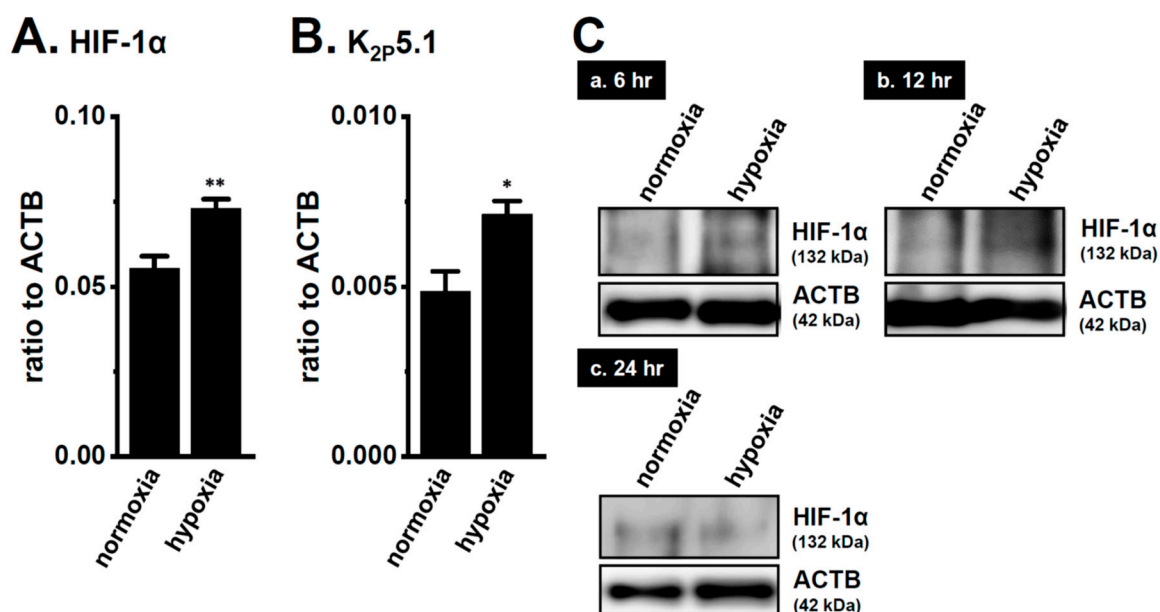


Figure 2. Up-regulation of the two-pore domain K⁺ channel (K_{2p})5.1 by hypoxia for 12 h in the concanavalin-A (Con-A)-stimulated splenic CD4⁺ T cells of mice. Real-time PCR assay for HIF-1α (A) and K_{2p}5.1 (B) in splenic CD4⁺ T cells exposed to hypoxic conditions (1.5% O₂) (*n* = 4 mice). Expression levels are shown as a ratio to ACTB. (C) HIF-1α protein expression (132 kDa) in splenic CD4⁺ T cells exposed to hypoxic conditions for 6 (a), 12 (b), and 24 (c) h. Protein lysates of the examined cells were probed by immunoblotting with anti-HIF-1α (upper panel) and anti-ACTB (42, kDa, lower panel) antibodies on the same filter. Results are expressed as means ± SEM. *, **: *p* < 0.05, 0.01 vs. normoxia.

In order to show the hypoxia-exposed up-regulation of K_{2p}5.1 proteins in stimulated CD4⁺ T cells, we then performed a functional analysis of K_{2p}5.1 activity. As reported in our previous studies [9,29], K_{2p}5.1 activity in mouse splenic CD4⁺ T cells can be estimated as alkaline pH-induced hyperpolarizing responses [a decrease in the fluorescence intensity of the voltage-sensitive fluorescent dye, bis-(1,3-dibutylbarbituric acid)trimethine oxonol, DiBAC₄(3)]. Corresponding to greater increases in K_{2p}5.1 expression under hypoxic conditions, the alkaline pH (pH 8.5 from pH 7.4)-induced hyperpolarizing responses were significantly larger in the hypoxia-exposed CD4⁺ T cells than in the normoxia-exposed cells (*p* = 0.0350) (Figure 3A,B). A pretreatment with clofilium (5 μM), a non-selective but potent K_{2p}5.1 blocker, prevented alkaline pH-induced hyperpolarizing responses (Figure S2), as reported in a previous study [9]. A similar up-regulation of K_{2p}5.1 with an increase in the expression of HIF-1α under hypoxic conditions was observed in Con-A-stimulated mouse thymocytes (*p* = 0.0005 and *p* = 0.0170 in HIF-1α and K_{2p}5.1, respectively) (Figure 4A,B), as well as the K_{2p}5.1-expressing mouse T-lymphocyte cell line, mCTLL-2 cells (*p* = 0.0084 and *p* = 0.0000 for HIF-1α and K_{2p}5.1, respectively) (Figure 4C,D). Correspondingly, alkaline pH-induced hyperpolarizing responses were significantly larger in the hypoxia-induced mCTLL-2 cells (Figure 5A,B) than in the normoxia-exposed cells (*p* = 0.0000).

Recent studies have shown that hypoxia-induced alternative splicing events in cancerous cells [30,31]. We identified an N terminus-lacking, dominant-negative, spliced isoform of K_{2p}5.1 in lymphoid cells [32], and we also found that a pre-mRNA inhibitor, pladienolide B, induced the down-regulation of functional, full-length K_{2p}5.1 and the up-regulation of the non-functional spliced

isoform (transcript variant X1) lacking three transmembrane domains and the first pore domain [29]. In the hypoxia-exposed CD4⁺ T cells, a full-length K_{2p}5.1 with a molecular weight of approximately 1.7 kbp, was identified by DNA sequencing, but the spliced isoforms of K_{2p}5.1 with molecular weights of less than 1 kbp were not. These results suggest that the dysregulated splicing of K_{2p}5.1 is not involved in inflammation-associated hypoxia-induced enhancements in K_{2p}5.1 activity in IBD model mice.

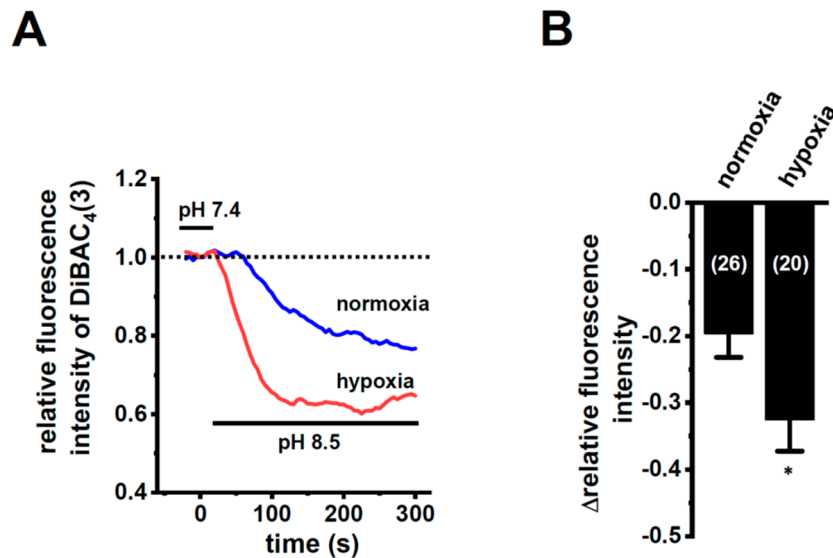


Figure 3. Enhanced K_{2p}5.1 activity by hypoxia for 24 h in stimulated splenic CD4⁺ T cells of mice. (A) Time course of voltage-sensitive fluorescent dye imaging of alkaline-pH (pH 8.5)-induced hyperpolarizing responses in splenic CD4⁺ T cells. The fluorescent intensity of DiBAC₄(3) before the change in pH from 7.4 to 8.5 (at 0 s) is expressed as 1.0. Images were measured every 5 s. (B) Summarized results of alkaline pH-induced hyperpolarizing responses. Cells were isolated from four different mice in each group. Cell numbers used in experiments are shown in parentheses. The values for fluorescent intensity were obtained by measuring the average for 1 min (12 images). Results are expressed as means ± SEM. *: $p < 0.05$ vs. normoxia.

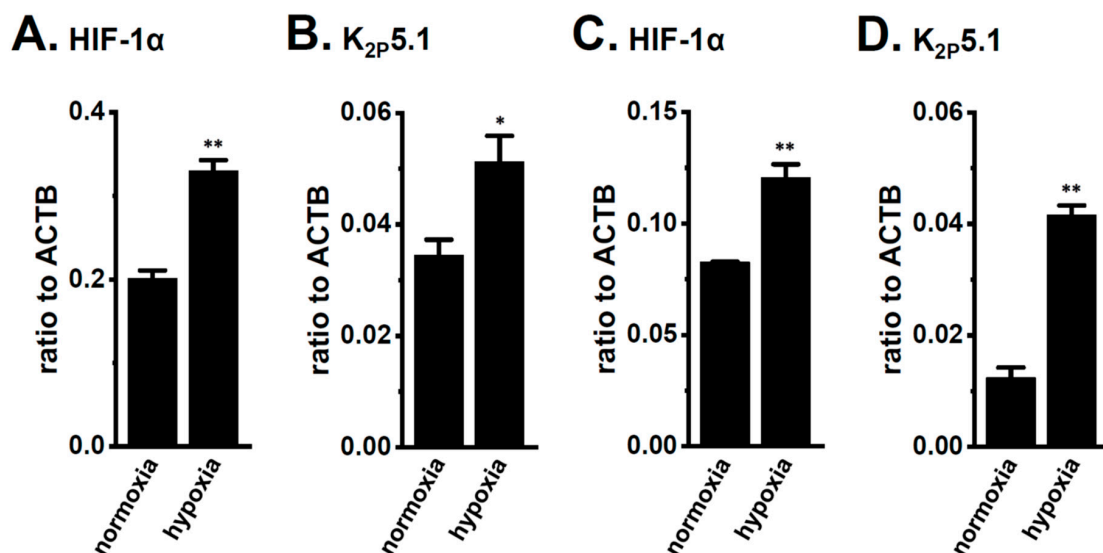


Figure 4. Up-regulation of HIF-1 α and K_{2p}5.1 by hypoxia (1.5% O₂) for 24 h in the stimulated thymocytes of mice and the mouse T-cell line mCTLL-2. Real-time PCR assay for HIF-1 α (A,C) and K_{2p}5.1 (B,D) in stimulated thymocytes (A,B) and mCTLL-2 cells (C,D) exposed to hypoxic conditions ($n = 4$). Expression levels are shown as a ratio to ACTB. Results are expressed as means ± SEM. *, **: $p < 0.05, 0.01$ vs. normoxia.

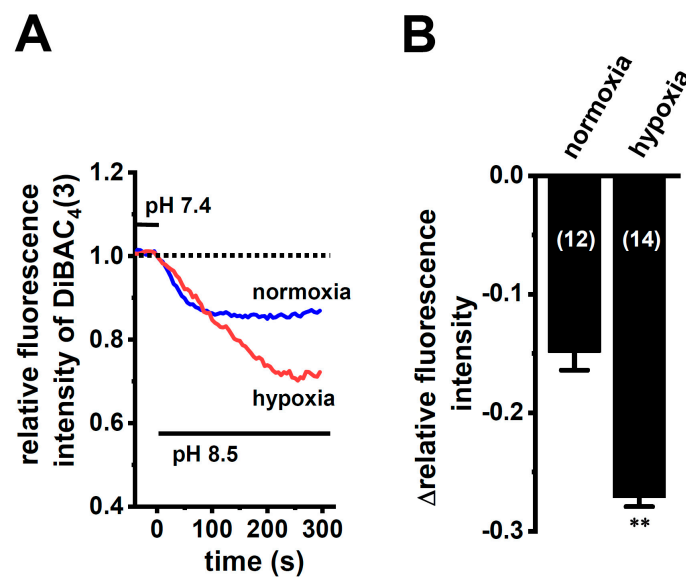


Figure 5. Enhanced $K_{2p5.1}$ activity by hypoxia for 24 h in mCTLL-2 cells. (A) Time course of voltage-sensitive fluorescent dye imaging of alkaline-pH (pH 8.5)-induced hyperpolarizing responses in normoxia- and hypoxia-exposed mCTLL-2 cells. The fluorescent intensity of DiBAC₄(3) before the change in pH from 7.4 to 8.5 (at 0 s) is expressed as 1.0. Images were measured every 5 s. (B) Summarized results of voltage-sensitive fluorescent dye imaging of alkaline-pH-induced hyperpolarizing responses in normoxia- and hypoxia-exposed mCTLL-2 cells. Cell numbers used in experiments are shown in parentheses. Results are expressed as means \pm SEM. **: $p < 0.01$ vs. normoxia.

2.3. Effects of the HIF Inhibitor on $K_{2p5.1}$ Expression and Activity in Stimulated Splenic $CD4^+$ T Cells

We examined the effects of the treatment with 1 μ M of FM19G11, an HIF inhibitor, for 24 h on $K_{2p5.1}$ expression and activity in hypoxia-exposed splenic $CD4^+$ T cells. As shown in Figure 6A, $K_{2p5.1}$ transcripts were significantly decreased by the FM19G11 treatment ($n = 4$, $p = 0.0127$). Correspondingly, alkaline pH (pH 8.5)-induced hyperpolarizing responses were reduced by the FM19G11 treatment ($p = 0.0238$) (Figure 6B,C). On the other hand, no significant changes in the $K_{2p5.1}$ expression ($p = 0.8294$) were found by the treatment with a selective HIF-2 inhibitor, HIF-2 antagonist 2 (HIF-2 inh, 10 μ M) [33] ($n = 4$) (Figure 6D). These results suggest that $K_{2p5.1}$ transcription is regulated by HIF-1 in T cells.

2.4. Effects of the Class III Histone Deacetylase SIRT1 Inhibitor NCO-01 on $K_{2p5.1}$ Expression and Activity in Stimulated $CD4^+$ Cells

Our previous findings indicated that the up-regulation of class I HDACs (HDAC2 and HDAC3) contributed to the increased expression and activity of $K_{Ca}3.1$ in the $CD4^+$ cells of the IBD model mice; however, class I HDAC inhibitor-induced decreases in the expression levels of $K_{2p5.1}$ transcripts were not found [13]. Recent studies have revealed down-regulated sirtuin-1 (SIRT1) in IBD patients and model mice [27] and reduced SIRT1 activity by the down-regulation of NAD⁺ [34,35]. No significant changes were observed in the expression levels of $K_{2p5.1}$ transcripts ($n = 4$, $p = 0.6124$) (Figure 7A) in the splenic $CD4^+$ T cells of IBD model mice, treated with 1 μ M of vorinostat, a pan-HDAC inhibitor, and 50 μ M of NCO-01, an SIRT1/2 inhibitor for 24 h. NCO-01 inhibits SIRT1 activity with a half maximal inhibitory concentration value of approximately 50 μ M [36]. The trypan blue dye exclusion test indicated $72.6 \pm 6.4\%$ and $70.5 \pm 2.7\%$ viable cells 24 h after the vehicle and NCO-01 treatments, respectively ($p = 0.7376$). Similarly, the expression level of $K_{2p5.1}$ transcripts was not affected by the treatment with NCO-01 in stimulated thymocytes ($n = 4$, $p > 0.05$) (Figure 7B) or mCTLL-2 cells ($n = 4$, $p > 0.05$) (Figure 7C).

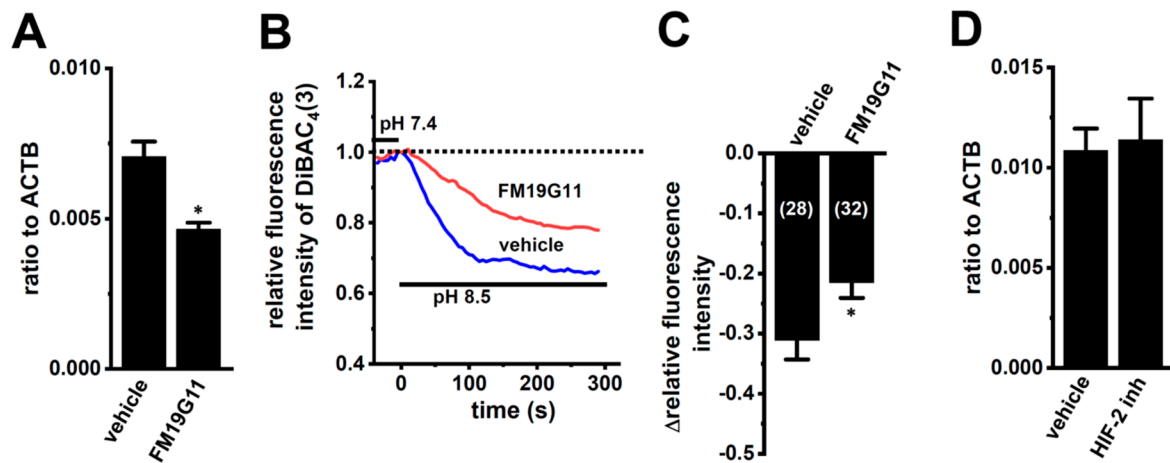


Figure 6. Decreased $K_{2p}5.1$ expression level and activity by the pharmacological inhibition of HIF in hypoxia-exposed splenic $CD4^+$ T cells. (A,D) Real-time PCR assay for $K_{2p}5.1$ in hypoxia-exposed splenic $CD4^+$ T cells that were treated with a vehicle, FM19G11 (1 μ M) (A), and HIF-2 antagonist 2 (HIF-2 inh.) (10 μ M) (D) for 24 h ($n = 4$). Expression levels are shown as a ratio to ACTB. (B) Voltage-sensitive fluorescent dye imaging of alkaline pH (pH 8.5)-induced hyperpolarizing responses in the vehicle- and FM19G11-treated groups. The fluorescent intensity of DiBAC₄(3) before the change in pH from 7.4 to 8.5 at 0 s is expressed as 1.0. Images were measured every 5 s. (C) Summarized results of alkaline pH-induced hyperpolarizing responses in the vehicle- and FM19G11-treated groups. Cells were isolated from four different mice in each group. Cell numbers used in experiments are shown in parentheses. The values for fluorescent intensity were obtained by measuring the average for 1 min (12 images). Results are expressed as means \pm SEM. *: $p < 0.05$ vs. vehicle control.

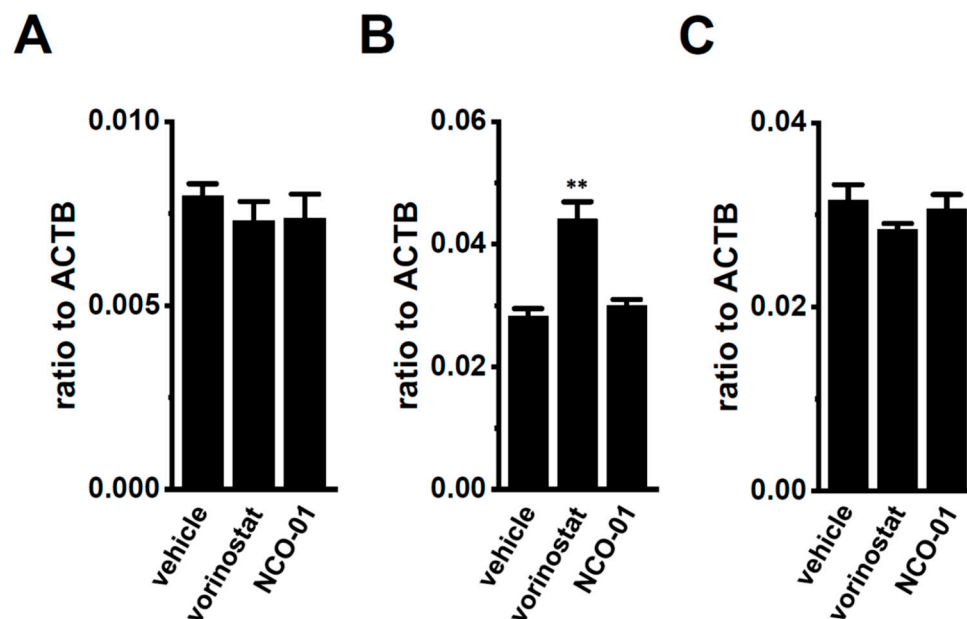


Figure 7. No significant changes in $K_{2p}5.1$ expression by the pharmacological inhibition of sirtuin-1 (SIRT1) in the splenic $CD4^+$ T cells of IBD model mice and the T-cell lineage. (A–C) Real-time PCR assay for $K_{2p}5.1$ in the splenic $CD4^+$ T cells of IBD model mice (A), stimulated thymocytes (B), and mCTLL-2 cells (C), all of which were treated with a vehicle, vorinostat (1 μ M), and NCO-01 (50 μ M) for 24 h [$n = 4$ mice (A,B) and $n = 4$ batches (C)]. Expression levels are shown as a ratio to ACTB. Results are expressed as means \pm SEM. **: $p < 0.01$ vs. vehicle control.

2.5. No Acute Compensatory Responses of $K_{2P3.1}$ to $K_{2P5.1}$ Up-Regulation in $CD4^+$ T Cells of IBD Model Mice and Hypoxia-Exposed T Cells

Bittner et al. (2015) showed the compensatory up-regulation of $K_{2P3.1}$ in $K_{2P5.1}$ -deficient mice [37]. In our previous study that used 7 week-old mice, the expression levels of $K_{2P3.1}$ in the splenic $CD4^+$ T cells of both the wild-type $K_{2P5.1}^{+/+}$ and homozygous $K_{2P5.1}$ knockout $K_{2P5.1}^{-/-}$ mice were low, and alkaline pH (pH 8.5)-induced hyperpolarizing responses were not detected (Figure 8A,B). Further study revealed increases in $K_{2P3.1}$ expression and activity in the splenic $CD4^+$ T cells of $K_{2P5.1}^{-/-}$ mice older than 13 weeks. In the 20-week-old $K_{2P5.1}^{-/-}$ mice, marked increases were observed in $K_{2P3.1}$ expression ($p = 0.0001$) (Figure 8A) and activity ($p = 0.0000$) (Figure 8B,C). The expression levels of other pH-sensitive K_{2P} channel subtypes, the $K_{2P9.1}$ (TASK-3/KCNK9) and $K_{2P16.1}$ (TALK-1/KCNK16) transcripts were very low (<0.001 in arbitrary units) in the $CD4^+$ T cells of the $K_{2P5.1}^{-/-}$ mice, and no significant changes were observed between the $K_{2P5.1}^{+/+}$ and $K_{2P5.1}^{-/-}$ mice. In comparisons with the expression levels of $K_{2P5.1}$, those of $K_{2P3.1}$ were markedly lower in the $CD4^+$ T cells, and no significant differences were found between the normal and IBD model mice ($n = 4$, $p = 0.1252$) (Figure 9A). Similar results were obtained in the hypoxia-exposed splenic $CD4^+$ T cells (Figure 9B), thymocytes (Figure 9C), and mCTL-2 cells (Figure 9D) ($n = 4$ mice (Figure 9B,C) and $n = 4$ batches (Figure 9D), $p = 0.7393$, 0.7799 , and 0.9229 , respectively). These results indicate that the alternations observed in $K_{2P5.1}$ expression and activity in T cells in the present study were not accompanied by the compensation of $K_{2P3.1}$.

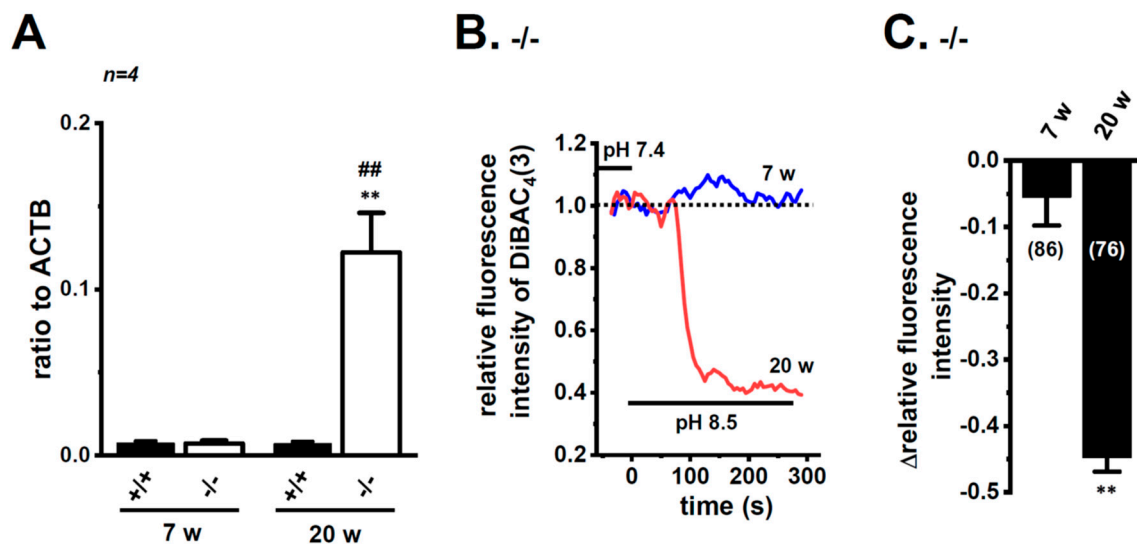


Figure 8. Compensatory increase in $K_{2P3.1}$ expression and activity in the splenic $CD4^+$ T cells of adult $K_{2P5.1}$ homozygous knockout (KO) mice. (A) Real-time PCR assay for $K_{2P3.1}$ in the splenic $CD4^+$ T cells of wild-type ($K_{2P5.1}^{+/+}$) and $K_{2P5.1}$ homozygous KO ($K_{2P5.1}^{-/-}$) mice at 7 (young) and 20 (adult) weeks old ($n = 4$). Expression levels are shown as a ratio to ACTB. (B) Voltage-sensitive fluorescent dye imaging of alkaline pH (pH 8.5)-induced hyperpolarizing responses in the splenic $CD4^+$ T cells of $K_{2P5.1}^{-/-}$ mice at 7 and 20 weeks. The fluorescent intensity of DiBAC₄(3) before the change in pH from 7.4 to 8.5 (at 0 s) is expressed as 1.0. Images were measured every 5 s. (C) Summarized results of alkaline pH (pH 8.5)-induced hyperpolarizing responses in the splenic $CD4^+$ T cells of $K_{2P5.1}^{-/-}$ mice at 7 and 20 weeks. Cells were isolated from three different mice in each group. Cell numbers used in experiments are shown in parentheses. Results are expressed as means \pm SEM. **: $p < 0.01$ vs. 7 weeks, $K_{2P5.1}^{-/-}$, #: $p < 0.01$ vs. 20 weeks, $K_{2P5.1}^{+/+}$.

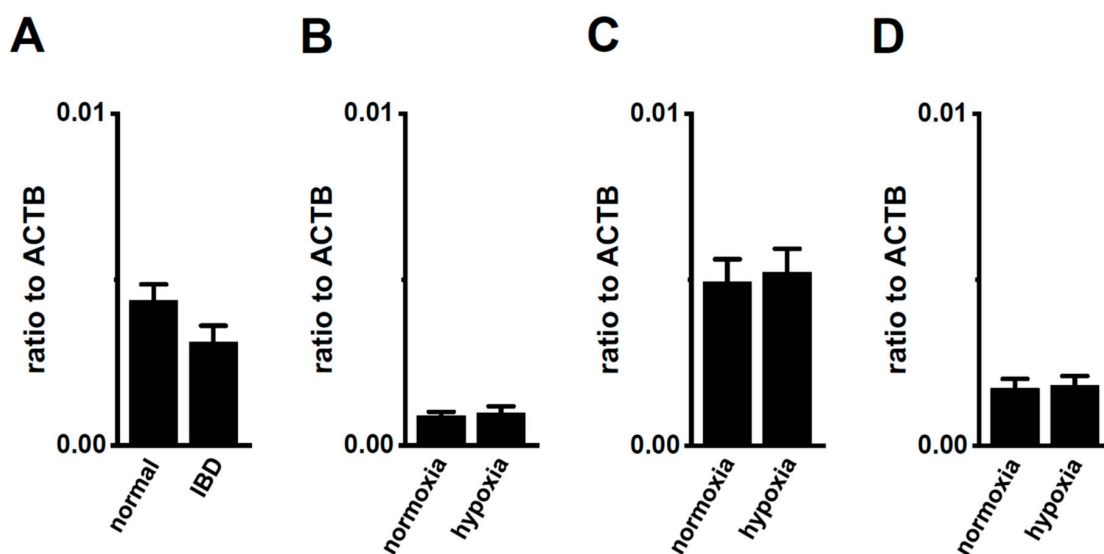


Figure 9. No compensatory changes in the expression levels of $K_{2p3.1}$ transcripts in the splenic $CD4^+$ T cells of IBD model mice or hypoxia-exposed T cells. (A–D) Real-time PCR assay for $K_{2p3.1}$ in the splenic $CD4^+$ T cells of ‘normal’ and ‘IBD’ model mice (A), hypoxia-exposed splenic $CD4^+$ T cells (B), hypoxia-exposed thymocytes (C), and hypoxia-exposed mCTLL-2 cells (D) ($n = 4$ mice (A–C) and $n = 4$ batches (D)). Expression levels are shown as a ratio to ACTB. Results are expressed as means \pm SEM.

3. Discussion

IFN- γ production was increased by the activation of the background $K_{2p5.1}$ K^+ channel function with its up-regulation in the $CD4^+$ T cells of the IBD model mice, and most IBD symptoms were decreased in the $K_{2p5.1}$ knockout mice [9]. Hypoxia is one of the crucial factors for an inflammatory microenvironment in autoimmune diseases, including IBD. Hypoxia-mediated signaling is involved in the pathogenesis of IBD by promoting an intestinal inflammatory response [17,18]. The main results of the present study are as follows: (1) Significant increases in HIF-1 α were seen in the inflammatory $CD4^+$ T cells of the IBD model mice that were isolated from a secondary lymphoid tissue, the spleen (Figure 1), (2) the HIF-1-mediated up-regulation of $K_{2p5.1}$ was seen in stimulated $CD4^+$ T cells (Figures 2, 3, 5 and 6), and (3) no involvement of the class III HDAC, SIRT1, was in the post-translational modifications to $K_{2p5.1}$ in these cells (Figure 7). Hypoxia-mediated up-regulation and the absence of SIRT1-mediated post-translational modifications to $K_{2p5.1}$ were noted in other T-cell lineages (Figures 4, 5 and 7). Previous studies have shown that the dominant-negative spliced isoform of $K_{2p5.1}$ prevents $K_{2p5.1}$ activity by inhibiting the plasma membrane trafficking of dimeric channel assembly [29,38]. Under hypoxic conditions, no increase was noted in the expression level of the dominant-negative isoform of $K_{2p5.1}$ in stimulated $CD4^+$ T cells.

The alkaline pH-activated K_{2p} channel subfamily is composed of three members: $K_{2p5.1}$ /TASK2, $K_{2p16.1}$ /TALK2, and $K_{2p17.1}$ /TALK2, while the mouse homologue of $K_{2p17.1}$ has not been molecularly identified. Furthermore, the acidic pH-sensitive K_{2p} channel subfamily, TASK ($K_{2p3.1}$ /TASK1 and $K_{2p9.1}$ /TASK3) also showed an increased channel activity with an alkaline pH stimulation. In stimulated $CD4^+$ T cells, the expression of these K_{2p} subtypes, except for $K_{2p5.1}$, was very weak, and no significant changes in their expression levels were observed following exposure to hypoxia. Similar to a recent study by Bittner et al. (2015) [37], $K_{2p3.1}$ was up-regulated in the splenic $CD4^+$ T cells of the ‘adult’ $K_{2p5.1}$ homozygous knockout mice (Figure 8). The expression levels of $K_{2p3.1}$ transcripts were markedly lower than those of $K_{2p5.1}$ in the T-cell lineage, and these levels were not changed by the exposure to hypoxia (Figure 9). These results suggest that the alkaline pH-induced hyperpolarizing responses observed in the present study were mainly due to the activation of $K_{2p5.1}$.

The transcriptional response to hypoxia is mainly mediated by epigenetic and post-translational modifications [39]. High levels of histone acetylation have been detected in biopsies from IBD patients

and IBD model mice, and HDACs play an important role as regulators of inflammation. HDAC inhibitors decrease disease severity by suppressing inflammatory cytokine production in IBD model mice [40]. $K_{Ca}3.1$, one of the major subtypes of K^+ channels in T cells, was found to be up-regulated in the $CD4^+$ T cells of IBD model mice [41]. We recently reported that $K_{Ca}3.1$, but not $K_{2P}5.1$, was regulated by the class I HDACs, HDAC2 and HDAC3 in activated $CD4^+$ T cells [13]. Conversely, the HIF-1-downstream molecule SIRT1 was down-regulated in IBD patients and model mice [27]. As shown in Figure 7, the treatment with the SIRT1 inhibitor did not alter $K_{2P}5.1$ transcription in the stimulated $CD4^+$ T cells or the T-cell lineage. Therefore, in addition to class I HDACs, SIRT1 does not appear to be a post-translational regulator of $K_{2P}5.1$ in the $K_{2P}5.1$ -overexpressing $CD4^+$ T cells of IBD model mice.

The HIF-1 dimer binds to the target HIF-1-responsive element (HRE) region in order to activate target gene transcription [42]. Brazier et al. (2005) [43] cloned the $K_{2P}5.1$ promoter, the activity of which is sensitive to oxygen, and the consensus binding sites for ETS (E-twenty six)-like 1 (Elk-1) were essential for transcriptional promotion by $K_{2P}5.1$. Elk-1 may physically interact with HIF-1 α . On the other hand, Cesari et al. (2004) showed that an Elk-1 deficiency did not induce changes in the proteomic displays of spleen extracts, and there were no immunological defects [44]. Shin et al. (2014) demonstrated that $K_{2P}5.1$ was up-regulated under hypoxic conditions in an HIF-1 α -dependent manner in B cells [24]. However, the underlying mechanisms of the HIF-1 α -mediated up-regulation of $K_{2P}5.1$ have not yet been elucidated. Under hypoxic conditions, the phosphorylation of STAT3 is increased in Th1 cells and leads to HIF-1 α transcription [45]. Therefore, the hypoxia-induced activation of the STAT3 signaling pathway may be involved in the up-regulation of $K_{2P}5.1$ in T cells. We examined the effects of treatments with STAT3 inhibitors (10 μ M static, Abcam, Cambridge, UK) for 12 h on the expression levels of $K_{2P}5.1$ transcripts in Con-A-stimulated splenic $CD4^+$ T cells. However, the STAT3 inhibitor treatment caused cell death, and, thus, we were unable to measure the expression or activity of $K_{2P}5.1$. This may be attributed to a defect in Con-A-induced T cell proliferation because the Con-A-induced phosphorylation of STAT3 promotes cell viability via the STAT3 signaling pathway [46]. The systematic evaluation of gene expression and DNA methylation in The Cancer Genome Atlas indicated the involvement of the hypomethylation of specific CpG loci with $K_{2P}5.1$ overexpression in triple-negative breast cancer patients [47]. Genome- and epigenome-wide analyses of IBD [48,49] have systematically assessed the transcriptional and post-translational mechanisms underlying the up-regulation of $K_{2P}5.1$ in T cells. $K_{2P}5.1$ partners (such as 14–3–3 isoforms), stabilized protein expression, and promoted the plasma membrane trafficking of channel assembly [50]. Additionally, interactions between $K_{2P}5.1$ and 14–3–3 may increase under hypoxic conditions. These findings suggest that increases in the interaction between 14–3–3 and $K_{2P}5.1$ under inflammation-associated hypoxic conditions may be at least partly involved in enhancements in $K_{2P}5.1$ activity in IBD.

The HIF-1 α stimulation under inflammation-associated hypoxic conditions promotes $CD4^+$ T cells to convert to regulatory T (T_{reg}) cells, which produce the anti-inflammatory cytokine interleukin (IL)-10, and this plays an important role in protection against IBD [51]. The up-regulation of $K_{2P}5.1$ with increases in HIF-1 α expression was observed in the splenic $CD4^+CD25^+$ T cells of the IBD model mice (Figure S3A–C). These results suggest that $K_{2P}5.1$ plays a role in the differentiation into T_{reg} cells and induction of IL-10. We previously reported that the Con-A stimulation converted splenic $CD4^+$ T cells to $CD4^+CD25^{high}Foxp3^{high}$ cells [29]. HIF-1 α activates Foxp3 transcription in T_{reg} cells [51]. However, no significant changes were found in the expression levels of Foxp3 following the treatment with a potent but non-selective $K_{2P}5.1$ blocker, clofilium, in Con-A-stimulated $CD4^+$ T cells ($p = 0.2566$) (Figure S3D), thus suggesting that $K_{2P}5.1$ activation is not involved in the differentiation into Foxp3 $^+$ T_{reg} cells. This issue is not the main subject of the present study, and, thus, further studies are needed to elucidate the physiological and pathophysiological roles of $K_{2P}5.1$ channels in T_{reg} cells.

4. Materials and Methods

4.1. Preparation of the DSS-Induced Mouse Model of IBD and Isolation of CD4⁺ T Cells

Male C57 black 6 Jackson (C57BL/6J, 5–6 weeks of age) mice (Japan SLC, Shizuoka, Japan) were acclimatized for 1 week before the experiment. They were given drinking water containing 5% (*w/v*) DSS 5000 (Fujifilm Wako Pure Chemical, Osaka, Japan) *ad libitum* [9,13]. Like our previous study [9,13], male mice developed more significant and aggressive diseases than female ones [52]. Control mice were given drinking water only. Seven days after the administration of DSS, mice were euthanized, their spleens were isolated, and their symptoms like colitis and colonic inflammation were assessed, as described in our previous study [9,13]. All experiments were performed in accordance with the Guiding Principles for the Care and Use of Laboratory Animals in Nagoya City University (NCU) and Kyoto Pharmaceutical University (KPU) with the approval of the presidents (No. H29M-50, NCU; No. 16-12-091, KPU). K_{2p}5.1 heterozygous knockout mice (K_{2p}5.1^{+/-}) that were bred in a C57BL6 background [B6; CB-Kcnk5Gt(pU-21)81Imeg] were purchased from the Center for Animal Resource and Development (CARD) (Kumamoto University, Kumamoto, Japan). Homozygous (K_{2p}5.1^{-/-}) knockout (KO) mice were generated by crossing K_{2p}5.1^{+/-} males with K_{2p}5.1^{+/-} females [9]. Genomic DNA isolation and RT-PCR were performed to distinguish the K_{2p}5.1 wild type and gene-trapped KO mice, as described in our previous study [9].

Single-cell suspensions were prepared by pressing the spleen or thymus with a frosted glass slide and then filtering them through cell strainers. CD4⁺CD25⁻ or CD4⁺ T cells were isolated from cell suspensions by using the Dynabeads FlowComp mouse CD4⁺CD25⁺ or CD4⁺ kit according to the experimental manual supplied by Thermo Fisher Scientific (Waltham, MA, USA). Flow cytometric analyses confirmed that 95% of purified T cells were CD4⁺CD25⁻ or CD4⁺. Oxygen levels in culture media were adjusted with oxygen-absorbing packs (Mitsubishi Gas Chemical, Tokyo, Japan) and monitored by an oxygen monitor (Oxy-M, Jikco limited, Tokyo, Japan) by using the BIONIX hypoxic culture kit (Sugiyamagen, Tokyo, Japan).

4.2. Cell Culture

The mCTLL-2 was supplied by the RIKEN BioResource Center (RIKEN BRC) (Tsukuba, Japan). Cells were maintained at 37 °C, in 5% CO₂ with an RPMI 1640 medium (FUJIFILM Wako Pure Chemical) supplemented with 10% fetal bovine serum (Sigma-Aldrich, St. Louis, MO, USA), a penicillin-streptomycin mixture (FUJIFILM Wako Pure Chemical), and 100 U/mL of IL-2 (Sigma-Aldrich).

4.3. RNA Extraction, Reverse Transcription (RT)-PCR, and Real-Time PCR

Total RNA extraction and RT-PCR from mouse splenic CD4⁺ T cells and mCTLL-2 cells were performed as previously reported [9,13]. The resulting complementary DNA (cDNA) products were amplified with gene-specific primers that were designed by Primer Express software (ver. 3.0.1, Thermo Fisher Scientific). Quantitative real-time PCR was performed by using Sybr Green Chemistry (SYBR Premix Ex Taq II) (TaKaRa BIO, Osaka, Japan) on the ABI 7500 Fast real-time PCR instrument (Thermo Fisher Scientific), as previously reported [9,13]. The following PCR primers for mouse clones were used for real-time PCR: K_{2p}5.1 (GenBank accession number: NM_021542, 792–921), 130 bp; hypoxia-inducible factor (HIF)-1 α (NM_010431, 963–1062), 100 bp; HIF-2 α (NM_010137, 737–856), 120 bp; K_{2p}3.1 (NM_010608, 692–812), 121 bp; K_{2p}9.1 (NM_001033876, 757–877), 121 bp; K_{2p}16.1 (NM_029006, 192–312), 121 bp; β -actin (ACTB) (NM_007393, 418–518), 101 bp. Regression analyses of the mean values of multiplex RT-PCRs for log₁₀-diluted cDNA were used to generate standard curves. Unknown quantities relative to the standard curve for a particular set of primers were calculated, yielding the transcriptional quantitation of gene products relative to the endogenous standard, ACTB [9,13].

4.4. Molecular Cloning of $K_{2P5.1}$ from Mouse Splenic $CD4^+$ Cells

Gene-specific primers were designed based on the cloned mouse $K_{2P5.1}$ (NM_021542, 281–1971, 1691 bp). The obtained PCR products were ligated into pcDNA3.1(+)/Neo^r (Thermo Fisher Scientific), and DNA sequences were obtained by using a custom DNA sequencing service (Eurofins Genomics, Tokyo, Japan).

4.5. Western Blotting

Protein lysates were prepared from mouse $CD4^+$ T cells by using a lysis buffer for western blotting. After the quantification of protein concentrations by using the BIO-RAD DCTM protein assay, protein lysates were subjected to SDS-PAGE (10%). Blots were incubated with anti-HIF-1 α (28b) (Santa Cruz Biotechnology, Santa Cruz, CA, USA) and anti-ACTB (Sigma-Aldrich) antibodies, and they were then incubated with anti-mouse horseradish peroxidase-conjugated immunoglobulin G (IgG, Millipore, Temecula, CA, USA) [9,38]. An enhanced chemiluminescence detection system (Nacalai Tesque, Kyoto, Japan) was used to detect the bound antibody. The resulting images were analyzed by using Amersham Imager 600 (GE Healthcare Japan, Tokyo, Japan). The light intensities of the band signals relative to that of the ACTB signal were calculated by using ImageJ software (Ver. 1.42, NIH, Bethesda, MA, USA). In the summarized results, the relative protein expression levels in the control were expressed as 1.0.

4.6. Measurement of Membrane Potentials Using Fluorescent Voltage-Sensitive Dyes

Isolated splenic $CD4^+$ T cells were cultivated in an RPMI 1640 medium that was supplemented with 10% heat-inactivated fetal calf serum (Merck, Darmstadt, Germany), antibiotics (penicillin and streptomycin mixture, Fujifilm Wako Pure Chemicals), Con-A (5 μ g/mL), and IL-2 (10 U/mL) for 48 h. Membrane potentials were measured by using the voltage-sensitive dye DiBAC₄(3), as previously reported [9,38]. Changes induced in the fluorescent intensity of DiBAC₄(3) by alkaline pH (pH 8.5) were measured with an ORCA-Flash2.8 digital camera (Hamamatsu Photonics, Hamamatsu, Japan). Data collection and analyses were performed by using an HCImage system (Hamamatsu Photonics). Images were obtained every 5 s.

4.7. Chemicals

The sources of pharmacological agents were as follows: DiBAC₄(3) (Dojindo, Kumamoto, Japan), clofilium (Sigma-Aldrich), Con-A (Sigma-Aldrich), FM19G11 (Sigma-Aldrich), and HIF-2 antagonist 2 (SML0883, Sigma-Aldrich). The SIRT1/2 inhibitor NCO-01 was supplied by Drs. Suzuki and Elboray. All other agents were obtained from Sigma-Aldrich, Nacalai Tesque, and FUJIFILM Wako Pure Chemical.

4.8. Statistical Analysis

Statistical evaluation was performed with the statistical software XLSTAT (version 2013.1, Microsoft Japan, Tokyo, Japan). To determine the significance of differences between two groups and among multiple groups, the unpaired (except Figure 1D)/paired (Figure 1D alone) Student's *t* tests with Welch's correction or Tukey's tests were used. Results with *p* value of less than 0.05 or 0.01 were considered to be significant. Data are presented as means \pm SEM.

5. Conclusions

The present study demonstrated that 1) a hypoxic characteristic in inflamed colonic tissues generates HIF-1 α activation in the splenic $CD4^+$ T cells of IBD model mice, and 2) the $K_{2P5.1}$ channel is an HIF-1 α target gene in splenic $CD4^+$ T cells. Similar results were obtained in other T-cell lineage that were exposed to hypoxia. The present results suggest that post-translational modifications by class I and III HDACs are not involved in the transcriptional regulation of $K_{2P5.1}$ in $CD4^+$ T cells. A clearer understanding of the molecular mechanisms underlying the pathophysiological significance

of HIF-1 α -mediated K_{2p}5.1 regulation in IBD patients is needed, and this can be done by using genome-wide and epigenome-wide association studies on DNA methylation and microRNA. The functional roles of K_{2p}5.1 in the other T-cell subsets, such as T_{reg} cells, B cells, and myeloid cells, that are involved in the pathogenesis of IBD will provide valuable insights into autoimmune diseases.

Supplementary Materials: Supplementary materials can be found at <http://www.mdpi.com/1422-0067/21/1/38/s1>.

Author Contributions: K.E., S.T., and S.O. designed the study and wrote the initial draft of the manuscript. K.E., H.K., R.T., J.K., and S.O. contributed to data collection, analyses, and interpretation. E.E.E. and T.S. synthesized and quantitatively estimated HDAC inhibitors. All authors critically reviewed the manuscript, approved its final version, and agreed to be accountable for all aspects of the work in ensuring that questions related to the accuracy or integrity of any part of the work were appropriately investigated and resolved. All authors have read and agreed to the published version of the manuscript.

Funding: This research was funded by the following sources: JSPS KAKENHI Grant Number JP18KK0218 (SO), a JSPS Research Fellowship for Young Scientists Grant Number 17J09558 (KE), and the Salt Science Foundation (1723) (SO).

Acknowledgments: We thank Miki Matsui (Menicon Nect, Aichi, Japan) for technical assistance. Medical English Service (Kyoto, Japan) reviewed the manuscript prior to its submission.

Conflicts of Interest: The authors declare no conflict of interest. The funders had no role in the design of the study; in the collection, analyses, or interpretation of data; in the writing of the manuscript, or in the decision to publish the results.

References

1. Bittner, S.; Budde, T.; Wiendi, H.; Meuth, S.G. From the background to the spotlight: TASK channels in pathological conditions. *Brain Pathol.* **2010**, *20*, 999–1009. [[CrossRef](#)] [[PubMed](#)]
2. Feliciangeli, S.; Chatelain, F.C.; Bichet, D.; Lesage, F. The family of K_{2P} channels: Salient structural and functional properties. *J. Physiol.* **2015**, *593*, 2587–2603. [[CrossRef](#)] [[PubMed](#)]
3. Sepúlveda, F.V.; Pablo Cid, L.; Teulon, J.; Nimeyer, M.I. Molecular aspects of structure, gating, and physiology of pH-sensitive background K_{2P} and Kir K⁺-transport channels. *Physiol. Rev.* **2015**, *95*, 179–217. [[CrossRef](#)] [[PubMed](#)]
4. Cid, L.P.; Roa-Rojas, H.A.; Niemeyer, M.I.; González, W.; Araki, M.; Araki, K.; Sepúlveda, F. TASK-2: A K_{2P} K⁺ channel with complex regulation and diverse physiological functions. *Front. Physiol.* **2013**, *4*, 198. [[CrossRef](#)] [[PubMed](#)]
5. Williams, S.; Bateman, A.; O’Kelly, I. Altered expression of two-pore domain potassium (K_{2p}) channels in cancer. *PLoS ONE* **2013**, *8*, e74589. [[CrossRef](#)]
6. López-Cayuqueo, K.I.; Peña-Münzenmayer, G.; Niemeyer, M.I.; Sepúlveda, F.V.; Cid, F.V. TASK-2 K_{2P} K⁺ channel: Thoughts about gating and its fitness to physiological function. *Pflügers Arch.* **2015**, *467*, 1043–1053. [[CrossRef](#)]
7. Bittner, S.; Bobak, N.; Feuchtenberger, M.; Herrmann, A.M.; Göbel, K.; Kinne, R.W.; Hasen, A.J.; Budde, T.; Kleinschnitz, C.; Frey, O.; et al. Expression of K_{2p}5.1 potassium channels on CD4⁺ T lymphocytes correlates with disease activity in rheumatoid arthritis patients. *Arthritis Res. Ther.* **2011**, *13*, R21. [[CrossRef](#)]
8. Bittner, S.; Bobak, N.; Herrmann, A.M.; Göbel, K.; Meuth, P.; Höhn, K.G.; Stenner, M.P.; Budde, T.; Wiendl, H.; Meuth, S.G. Upregulation of K_{2p}5.1 potassium channels in multiple sclerosis. *Ann. Neurol.* **2010**, *68*, 58–69. [[CrossRef](#)]
9. Nakakura, S.; Matsui, M.; Sato, A.; Ishii, M.; Endo, K.; Muragishi, S.; Murase, M.; Kito, H.; Niguma, H.; Kurokawa, N.; et al. Pathological significance of the two-pore K⁺ channel K_{2p}5.1 in splenic CD4⁺CD25⁻ T cells subset from a chemically-induced murine inflammatory bowel disease model. *Front. Physiol.* **2015**, *6*, 299. [[CrossRef](#)]
10. Ohya, S.; Kito, H.; Hatano, N.; Muraki, K. Recent advances in therapeutic strategies that focus on the regulation of ion channel expression. *Pharmacol. Ther.* **2016**, *160*, 11–43. [[CrossRef](#)]
11. Feske, S.; Wulff, H.; Skolnik, E.Y. Ion channels in innate and adaptive immunity. *Annu. Rev. Immunol.* **2015**, *33*, 291–353. [[CrossRef](#)] [[PubMed](#)]
12. Vaeth, H.; Feske, S. Ion channelopathies of the immune system. *Curr. Opin. Immunol.* **2018**, *52*, 39–50. [[CrossRef](#)] [[PubMed](#)]

13. Matsui, M.; Terasawa, K.; Kajikuri, J.; Kito, H.; Endo, K.; Jaikhan, P.; Suzuki, T.; Ohya, S. Histone deacetylases enhance Ca²⁺-activated K⁺ channel K_{Ca}3.1 expression in murine inflammatory CD4⁺ cells. *Int. J. Mol. Sci.* **2018**, *19*, 2942. [[CrossRef](#)] [[PubMed](#)]
14. Ohya, S.; Kito, H. Ca²⁺-activated K⁺ channel K_{Ca}3.1 as a therapeutic target for immune disorders. *Biol. Pharm. Bull.* **2018**, *41*, 1158–1163. [[CrossRef](#)]
15. Marik, C.; Felts, P.A.; Bauer, J.; Lassmann, H.; Smith, K.J. Lesion genesis in a subset of patients with multiple sclerosis: A role for innate immunity. *Brain* **2007**, *130*, 2800–2815. [[CrossRef](#)]
16. Muz, B.; Khan, M.N.; Kiriakidis, S.; Paleolog, E.M. Hypoxia. The role of hypoxia and HIF-dependent signalling events in rheumatoid arthritis. *Arthritis Res. Ther.* **2009**, *11*, 201. [[CrossRef](#)]
17. Colgan, S.P.; Taylor, C.T. Hypoxia: An alarm signal during intestinal inflammation. *Nat. Rev. Gastroenterol. Hepatol.* **2010**, *7*, 281–287. [[CrossRef](#)]
18. Higashiyama, M.; Hokari, R.; Hozumi, H.; Kurihara, C.; Ueda, T.; Watanabe, C.; Tomita, K.; Nakamura, M.; Komoto, S.; Okada, Y.; et al. HIF-1 in T cells ameliorated dextran sodium sulfate-induced murine colitis. *J. Leukoc. Biol.* **2012**, *91*, 901–909. [[CrossRef](#)]
19. Taylor, C.T.; Colgan, S.P. Regulation of immunity and inflammation by hypoxia in immunological niches. *Nat. Rev. Immunol.* **2017**, *17*, 774–785. [[CrossRef](#)]
20. Flück, K.; Breves, G.; Fandrey, J.; Wining, S. Hypoxia-inducible factor 1 in dendritic cells is crucial for the activation of protective regulatory T cells in murine colitis. *Mucosal Immunol.* **2016**, *9*, 379–390. [[CrossRef](#)]
21. Deng, W.; Feng, X.; Li, X.; Wang, D.; Sun, L. Hypoxia-inducible factor 1 in autoimmune diseases. *Cell. Immunol.* **2016**, *303*, 7–15. [[CrossRef](#)] [[PubMed](#)]
22. Bäcker, V.; Cheung, F.Y.; Siveke, J.T.; Fandray, J.; Winning, S. Knockdown of myeloid cell hypoxia-inducible factor-1 α ameliorates the acute pathology in DSS-induced colitis. *PLoS ONE* **2017**, *12*, e0190074. [[CrossRef](#)] [[PubMed](#)]
23. Chimote, A.A.; Kuras, Z.; Conforti, L. Disruption of Kv1.3 channel forward vesicular trafficking by hypoxia in human T lymphocytes. *J. Biol. Chem.* **2012**, *287*, 2055–2067. [[CrossRef](#)] [[PubMed](#)]
24. Shin, D.H.; Lin, H.; Zheng, H.; Kim, K.S.; Kim, J.Y.; Chun, Y.S.; Park, J.W.; Nam, J.H.; Kim, W.K.; Zhang, Y.H.; et al. HIF-1 α -mediated upregulation of TASK-2 K⁺ channels augments Ca²⁺ signaling in mouse B cells under hypoxia. *J. Immunol.* **2014**, *193*, 4924–4933. [[CrossRef](#)]
25. Yuan, F.; Wang, H.; Feng, J.; Wei, Z.; Yu, H.; Zhang, X.; Zhang, Y.; Wang, S. Leptin signaling in the carotid body regulates a hypoxic ventilatory response through altering TASK channel expression. *Front. Physiol.* **2018**, *8*, 249. [[CrossRef](#)]
26. Chen, R.; Dioum, E.M.; Hogg, R.T.; Gerard, R.D.; Garcia, J.A. Hypoxia increases sirtuin 1 expression in a hypoxia-inducible factor-dependent manner. *J. Biol. Chem.* **2011**, *286*, 13869–13878. [[CrossRef](#)]
27. Caruso, R.; Marafini, I.; Franze, E.; Stolfi, C.; Zorzi, F.; Monteleone, I.; Caprioli, F.; Colantoni, A.; Sarra, M.; Sedda, S.; et al. Defective expression of SIRT1 contributes to sustain inflammatory pathways in the gut. *Mucosal Immunol.* **2017**, *7*, 1467–1479. [[CrossRef](#)]
28. Wellman, A.S.; Metukuri, M.R.; Kazgan, M.; Xu, X.; Xu, Q.; Ren, N.S.X.; Czopik, A.; Shanahan, M.T.; Kang, A.; Chen, W.; et al. Intestinal epithelial sirtuin 1 regulates intestinal inflammation during aging in mice by alter in the intestinal microbiota. *Gastroenterology* **2017**, *153*, 772–786. [[CrossRef](#)]
29. Tagishi, K.; Shimizu, A.; Endo, K.; Kito, H.; Niwa, S.; Fujii, M.; Ohya, S. Defective splicing of the background K_{2P}5.1 by the pre-mRNA splicing inhibitor, pladienolide B in lectin-activated mouse splenic CD4⁺ T cells. *J. Pharmacol. Sci.* **2016**, *132*, 205–209. [[CrossRef](#)]
30. Han, J.; Li, J.; Ho, J.C.; Chia, G.S.; Kato, H.; Jha, S.; Yang, H.; Poellinger, L.; Lee, K.L. Hypoxia is a key driver of alternative splicing in human breast cancer cells. *Sci. Rep.* **2017**, *7*, 4108. [[CrossRef](#)]
31. Kanopka, A. Cell survival: Interplay between hypoxia and pre-mRNA splicing. *Exp. Cell Res.* **2017**, *356*, 187–191. [[CrossRef](#)] [[PubMed](#)]
32. Kozako, T.; Suzuki, T.; Yoshimutsu, M.; Uchida, Y.; Kuroki, A.; Aikawa, A.; Honda, S.; Arima, N.; Soeda, S. Novel small-molecule SIRT1 inhibitors induce cell death in adult T-cell leukemia cells. *Sci. Rep.* **2015**, *5*, 11345. [[CrossRef](#)] [[PubMed](#)]
33. Hikage, F.; Atkins, S.; Kahana, A.; Smith, T.J.; Chun, T.H. HIF2A-LOX pathway promotes fibrotic remodeling in thyroid-associated orbitopathy. *Endocrinology* **2019**, *160*, 20–35. [[CrossRef](#)] [[PubMed](#)]
34. Lim, J.H.; Lee, Y.M.; Chun, Y.S.; Chen, J.; Kim, J.E.; Park, J.W. Sirtuin 1 modulates cellular responses to hypoxia by deacetylating hypoxia-inducible factor 1 α . *Mol. Cell* **2010**, *38*, 864–878. [[CrossRef](#)] [[PubMed](#)]

35. Leiser, S.F.; Kaeberlein, M. A role for SIRT1 in the hypoxic response. *Mol. Cell* **2010**, *38*, 779–780. [[CrossRef](#)] [[PubMed](#)]
36. Suzuki, T.; Imai, K.; Imai, E.; Iida, S.; Ueda, R.; Tsumoto, H.; Nakagawa, H.; Miyata, N. Design, synthesis, enzyme inhibition, and tumor cell growth inhibition of 2-anilinobenzamide derivatives as SIRT1 inhibitors. *Bioorg. Med. Chem.* **2009**, *17*, 5900–5905. [[CrossRef](#)]
37. Bittner, S.; Bobak, N.; Hofmann, M.S.; Schuhmann, M.K.; Ruck, T.; Gobel, K.; Bruck, W.; Wiendl, H.; Meuth, S.G. Murine K₂P5.1 deficiency has no impact on autoimmune neuroinflammation due to compensatory K₂P3.1- and K_v1.3-dependent mechanisms. *Int. J. Mol. Sci.* **2015**, *16*, 16880–16896. [[CrossRef](#)]
38. Endo, K.; Kurokawa, N.; Kito, H.; Nakakura, S.; Fujii, M.; Ohya, S. Molecular identification of the dominant-negative, splicing isoform of the two-pore domain K⁺ channel K₂P5.1 in lymphoid cells and enhancement of its expression by splicing inhibition. *Biochem Pharmacol.* **2015**, *98*, 440–452. [[CrossRef](#)]
39. Choudhry, H.; Harris, A.L. Advances in hypoxia-inducible factor biology. *Cell Metab.* **2018**, *27*, 281–298. [[CrossRef](#)]
40. Ali, M.N.; Chojjookhuu, N.; Takagi, H.; Srisowanna, N.; Nguyen, M.; Huynh, N.; Yamaguchi, Y.; Oo, P.S.; Kyaw, M.T.H.; Sato, K.; et al. The HDAC inhibitor, SAHA, prevents colonic inflammation by suppressing pro-inflammatory cytokines and chemokines in DSS-induced colitis. *Acta Histochem. Cytochem.* **2018**, *51*, 33–40. [[CrossRef](#)]
41. Ohya, S.; Fukuyo, Y.; Kito, H.; Shibaoka, R.; Matsui, M.; Niguma, H.; Maeda, Y.; Yamamura, H.; Fujii, M.; Kimura, K.; et al. Upregulation of K_{Ca}3.1 K⁺ channel in mesenteric lymph node CD4⁺ T lymphocytes from a mouse model of dextran sodium sulfate-induced inflammatory bowel disease. *Am. J. Physiol. Gastrointest. Liver Physiol.* **2014**, *306*, G873–G885. [[CrossRef](#)] [[PubMed](#)]
42. Loboda, A.; Jozkowicz, A.; Dulak, J. HIF-1 and HIF-2 transcription factors-similar but not identical. *Mol. Cells* **2010**, *29*, 435–442. [[CrossRef](#)] [[PubMed](#)]
43. Brazier, S.P.; Mason, H.S.; Bateson, A.N.; Kemp, P.J. Cloning of the human TASK-2 (KCNK5) promoter and its regulation by chronic hypoxia. *Biochem. Biophys. Res. Commun.* **2005**, *336*, 1251–1258. [[CrossRef](#)] [[PubMed](#)]
44. Cesari, F.; Bresht, S.; Ventersten, K.; Vuong, L.G.; Hofmann, M.; Klingel, K.; Schnorr, J.J.; Arsenian, S.; Schild, H.; Herdegen, T.; et al. Mice deficient for the ets transcription factor elk-1 show normal immune responses and mildly impaired neuronal gene activation. *Mol. Cell. Biol.* **2004**, *24*, 294–305. [[CrossRef](#)] [[PubMed](#)]
45. Shehade, H.; Acolty, V.; Moser, M.; Oldenhove, G. Cutting edge: Hypoxia-inducible factor 1 negatively regulates Th1 function. *J. Immunol.* **2015**, *195*, 1372–1376. [[CrossRef](#)] [[PubMed](#)]
46. Akla, N.; Platt, J.; Annabi, B. Concanavalin-A triggers inflammatory response through JAK/STAT3 signaling and modulates MT1-MMP regulation of COX-2 in mesenchymal stromal cells. *Exp. Cell Res.* **2012**, *318*, 2498–2506. [[CrossRef](#)]
47. Dookeran, K.A.; Zhang, W.; Stayner, L.; Argos, M. Associations of two-pore domain potassium channels and triple negative breast cancer subtype in the cancer genome atlas: Systematic evaluation of gene expression and methylation. *BMC Res. Notes* **2017**, *10*, 475. [[CrossRef](#)]
48. Ventham, N.T.; Kennedy, N.A.; Adams, A.T.; Kalla, R.; Heath, S.; O'leary, K.R.; Drummond, H.; Lauc, G.; Campbell, H.; McGovern, D.P.; et al. Satsangi, Integrative epigenome-wide analysis demonstrates that DNA methylation may mediate genetic risk in inflammatory bowel disease. *Nat. Commun.* **2016**, *7*, 13507. [[CrossRef](#)]
49. McDermott, E.; Ryan, E.J.; Tosetto, M.; Gibson, D.; Burrage, J.; Keegan, D.; Byrne, K.; Crowe, E.; Sexton, G.; Malone, K.; et al. DNA methylation profiling in inflammatory bowel disease provides new insights into disease pathogenesis. *J. Crohns Colitis* **2016**, *10*, 77–86. [[CrossRef](#)]
50. Fernández-Ort, J.; Ehling, P.; Ruck, T.; Pankratz, S.; Hofmann, M.S.; Landgraf, P.; Dieterich, D.C.; Smalla, K.H.; Kähne, T.; Seebohm, G.; et al. 14-3-3 proteins regulate K₂P5.1 surface expression on T lymphocytes. *Traffic* **2017**, *18*, 29–43. [[CrossRef](#)]

51. Clambey, E.T.; McNamee, E.N.; Westrich, J.A.; Glover, L.E.; Campbell, E.L.; Jedlicka, P.; de Zoeten, E.F.; Cambier, J.C.; Stenmark, K.R.; Colgan, S.P.; et al. Hypoxia-inducible factor-1 alpha-dependent induction of Foxp3 drives regulatory T-cell abundance and function during inflammatory hypoxia of the mucosa. *Proc. Natl. Acad. Sci. USA* **2012**, *109*, E2784–E2793. [[CrossRef](#)] [[PubMed](#)]
52. Chassaing, B.; Aitken, J.D.; Malleshappa, M.; Vijay-Kumar, M. Dextran sulfate sodium (DSS)-induced colitis in mice. *Curr. Protoc. Immunol.* **2014**, *104*, 15–25. [[CrossRef](#)] [[PubMed](#)]



© 2019 by the authors. Licensee MDPI, Basel, Switzerland. This article is an open access article distributed under the terms and conditions of the Creative Commons Attribution (CC BY) license (<http://creativecommons.org/licenses/by/4.0/>).